Energy and Environment Research; Vol. 4, No. 3; 2014
ISSN 1927-0569 E-ISSN 1927-0577
Published by Canadian Center of Science and Education

Mechanistic Study of the Wettability Modification in Carbonate and Sandstone Reservoirs during Water/Low Salinity Water Flooding

Zohreh Jalili[1] & Vahid Alipour Tabrizy[2]

[1] Department of Petroleum Engineering and Applied Geophysics, Norwegian University of Science and Technology, N7491, Trondheim, Norway

[2] Department of Reserve Replacements, Åsgard Petroleum Technology, Statoil ASA, Norway

Correspondence: Zohreh Jalili, Department of Petroleum Engineering and Applied Geophysics, Norwegian University of Science and Technology, N7491, Trondheim, Norway. Tel: 47-4674-7853. E-mail: zohrehj@stud.ntnu.no

Received: October 7, 2014 Accepted: October 16, 2014 Online Published: October 29, 2014

doi:10.5539/eer.v4n3p78 URL: http://dx.doi.org/10.5539/eer.v4n3p78

Abstract

The paper pertains to the analysis of the chemical interaction between sea water ions, asphaltene colloids and silicate /calcite mineral as a substrate during water/low salinity water flooding. The work tackles modeling of salinity dependent relative permeability and capillary pressure functions from contact angle to estimate oil recovery during water/low salinity water. The paper has two main parts. In the first part, static contact angle is calculated based on disjoining pressure and compared to the experimental values, reported in the literature. In the second part, the model is used to demonstrate that water film is more stable in presence of low salinity water compared to distilled water and sea water, for carbonate and silicate minerals. Increasing temperature enhances the stability of the water film around the substrate for both types of minerals. This could be future interpreted as an indication for extra oil recovery applying low salinity water injection at elevated temperature. It is interesting to observe from the model that, increasing the Mg^{2+} ion concentration enhances the hydrophilicity characteristics for calcite mineral modified by asphaltene while for silicate surface modified by asphaltene, SO_4^{2-} ion enhances the hydrophobicity behaviour.

Keywords: wettability alteration, calcite, quartz, magnesium, sulphate, low salinity water

Nomenclature

A	Hamaker constant (J)
A_s	Structural force coefficient (Pa)
e	electronic charge (=1.602×10^{-19} C)
h	Distance of separation (m)
h_s	Decay length (m)
J	Mean surface curvature
k	Boltzmann constant (1.38×10^{-23} m^2 kg s^{-2} K^{-1})
n	Refractive index of media
P_c	Capillary pressure (pa)
pH_0	Isoelectric point of the surface
r	Radius (m)
T	Absolute Temperature (K)
T_o	Reference Temperature (K)
V	Interaction potential (J)
ν_e	Plasma frequency of the free electron gas (3×10^{15} sec^{-1})
z	Ion valence

Greeks

δ	Collision diameter (m)
ε	Permittivity or dielectric constant of medium
$\hbar$	Plank constant (6.63×10^{-34} J/sec)
Φ	Surface potential (J)

κ Debye length (m)
λ Wave length (m)
Π Disjoining pressure (atm)
σ Surface/interfacial tension (N m^{-1})
θ Contact angle
ζ Zeta potential (V)

Subscripts

01 Mineral surface
02 Mineral surface
1 Solid
2 Oil phase
3 Aqueous phase (water film)
BR Born short range repulsive force
DLR Double layer electrostatic repulsive force
LVA London -Van der Waals attractive force
o Oil/original condition
w Water
p Particle

Abbreviations

DLVO Derjaguin, Landau, Verwey, Overbeek
DW Distilled water
LSW Low salinity water
Mg^{2+} Magnesium
SO_4^{2-} Sulfate
SSW Synthetic sea water
TDS Total dissolved solid

1. Introduction

Low salinity water-based enhanced oil recovery (EOR) has been recognized to contribute for extra oil recovery from sandstone reservoirs containing clay minerals in the literature (Lager et. al 2007 and Loahardjo et. al, 2007). In 2011, a laboratory study was documented for reservoir limestone cores from aqueous section of reservoir with two to five percentage of extra oil recovery by tertiary low salinity water injection (Austad et. al 2011). The experiments were performed by injection of formation water with salinity of 200000 ppm as a secondary recovery while the tertiary recovery was observed by injection of 100×diluted formation water or 10×diluted seawater (from Persian Gulf) at 110 °C (Austad et. al 2011). Migration of fines, double layer expansion and ionic exchange were seems to be the main hypothetical explanations for the efficiency of low salinity water flooding in sandstone reservoirs (Tang and Morrow1999; McGuire et al. 2005; Lager et al. 2007). Rezaei Doust et al. (2010) proposed a new chemical mechanism for Low salinity EOR based on wettability alteration by desorption of organic basic material form silicate minerals at specific range of pH. An increase of pH associated with flooding with low-salinity water (LSW) has been observed in the experimental work reported by Hamouda and Valderhaug (2014). It was observed by Hamouda and Valderhaug (2014) also that the pressure drop across the flooded cores with LSW is almost doubled of the pressure drop compared to cores flooded with SSW. They argued also low salinity brine will expand the electrical double layer as well as dissolution which will lead to fine detachment and mobilization; hence the sweep efficiency will be increased (Hamouda and Valderhaug 2014). Austad et al. (2011) also claimed that presence of anhydrite in limestone is necessary for enhanced oil recovery by low salinity water flooding in carbonates as the main mechanism is dissolution of anhydrite from mineral to ionic phase.

Hamouda and collogues in series of articles dealing with carbonate/silicate minerals, water and oil documented that the parameters that contributes the initial and final wetting condition, before and after imbibition, could be addressed as oil composition, ionic composition of irreducible and imbibing water, pH, rock surface characteristics and temperature (Alipour Tabrizy et al. 2011a; Alipour Tabrizy et al. 2011b; Petrovich and Hamouda 1998; Rezaei Gomari et al. 2006a; Rezaei Gomari et al. 2006c; Karoussi and Hamouda 2007; Hamouda and Karoussi 2008; Chukwudeme and Hamouda 2009). Several articles have been reported also in the literature on improving oil recovery by spontaneous and forced imbibition of seawater at high temperature

(>70 °C) (Cuie and Morrow 1991; Akin et al. 2000; Petrovich and Hamouda 1998; Babadagli 2003; Hirasaki and Zhang 2004; Rezaei Gomari et al. 2006a; Rezaei Gomari et al. 2006b; Karoussi and Hamouda 2007; Hamouda and Karoussi 2008; Chukwudeme and Hamouda 2009). It was reported also as the temperature increases, the degree of exchange of Mg^{2+} and SO_4^2 ions enhances (Karoussi and Hamouda 2007 and Petrovich and Hamouda 1998). Mahani et al. (2014) used a model of sandstone rock that consists of Na- Montmorillonite clay over glass substrate to observe the kinetic of oil droplet detachment in presence of low and high salinity water. They reported a wettability alteration process toward less oil-wet condition when the system is exposed to low salinity brine with slow kinetic reaction (Mahani et al. 2014). The field response to low salinity water flooding as secondary and tertiary modes were also addressed in another research work by Mahani et al. (2011). For one field, it was documented that dual step water cut is developed and the viscous force is the dominant mechanism which can be interpreted as a characteristic of change in wetting state; in contrast for another case study, the low salinity water flooding is immature and the breakthrough of low salinity brine was not yet observed due to strong bouncy effect caused by high vertical permeability of reservoir (Mahani et al. 2011).

In spite of the fact that several observations were reported for the application of low salinity water flooding in sandstone and carbonate rocks as a promising EOR technique, there are few reports in the literature to study oil recovery mechanism(s) associated to low salinity water injection applying universal mathematical model. This paper addresses the calculation of disjoining pressure and total interaction potentials of mineral/brine/asphaltene colloids linked to the effect of temperature, to study the influence of seawater ions and low salinity seawater on wettability modification of calcite and quartz surfaces. Static contact angle is calculated based on disjoining pressure and compared to the experimental values, reported previously in the literature by Alipour Tabrizy et al. (2011b). It is attempted also to generate oil/water relative permeability curves from calculated contact angle to investigate, the influences of sea water ions/low salinity water flooding on recovery process.

2. Theory

2.1 Fines Detachment by DLVO (Derjaguin Landau Verwy Overbeek) Theory

DLVO theory and experimental observations could indicate that fine detachment is the mechanism that may alter the wettability of the rock at high temperatures (Hamouda and Karoussi 2008). However, Hamouda and Karoussi (2008) did not provide any calculation of contact angle based on DLVO theory and simply used variation of disjoining pressure versus water film thickness to compare with imbibition and flooding experimental results. In DLVO theory, the interaction between particles (sphere-shape) and a pore surface is described by London van der Waals (LVA) attraction, double-layer repulsion (DLR) and Born repulsion (BR). The DLVO model may not be able to fully describe colloidal behavior in aqueous media. Grasoo et al. (2002) reviewed many of the interactions that play a role in environmental systems and are not commonly included by the traditional DLVO model: e.g., hydrogen bonding and the hydrophobic effect, hydration pressure, non-charge transfer Lewis acid base interactions, and steric interactions. They documented also that there are conflicting opinions in the literature as to whether steric interactions and other extended DLVO forces should be considered or not. While several studies have concluded that these contributions to be additive (Van Oss 1994; Jucker et al. 1998; Giasson et al. 1998 and Freitas et al. 2001); others disagree with this approach (e.g. Rijnaarts et al. 1999). It seems that the complexity of aqueous, hydrocarbon and oil system will most likely preclude the development of a unique approach that can be used for all conditions. In this work, hydration and structural forces are not taken into account for simplicity. Therefore the total interaction potentials (between a fine particle and mineral surface) may be expressed as follows (Israelachvili 1992):

$$V_t(h) = V_{LVA}(h) + V_{DLR}(h) + V_{BR}(h) \tag{1}$$

For a spherical particles and flat mineral surfaces, the interactions potential are expressed for the different interactions by the following equations (Israelachvili 1992):

$$V_{LVA}(h) = -\frac{A}{6}\left[\frac{2(H+1)}{H(H+2)} + \ln\left(\frac{H}{H+2}\right)\right] \tag{2}$$

where $H=h/r_p$; A is Hamaker constant; h is distance of separation; r_p is particle radius; ε is permittivity of medium (water); ε_0 is permittivity of free space; κ is Debye length and Φ_{01} and Φ_{02} are surface and particle surface potentials. Hamaker constant is calculated using Lifshitz theory as a function of temperature (Israelachvili 1992):

$$A = \frac{3}{4} k T \left(\frac{\varepsilon_1 - \varepsilon_3}{\varepsilon_1 + \varepsilon_3} \right) \left(\frac{\varepsilon_2 - \varepsilon_3}{\varepsilon_2 + \varepsilon_3} \right) + \frac{3\hbar \nu_e}{8\sqrt{2}} \frac{\left(n_1^2 - n_3^2 \right)^2 \left(n_2^2 - n_3^2 \right)^2}{\left(n_1^2 + n_3^2 \right)^{1/2} \left(n_2^2 + n_3^2 \right)^{1/2} \left\{ \left(n_1^2 + n_3^2 \right)^{1/2} + \left(n_2^2 + n_3^2 \right)^{1/2} \right\}} \tag{3}$$

Where, ε_1, ε_2 and ε_3 are the static dielectric constants of the three media, while n_1, n_2 and n_3 are values for the refractive index of media. K is Boltzmann constant (1.38×10^{-23} m^2 kg s^{-2} K^{-1}), T is temperature in Kelvin, $\hbar$ is Plank constant (6.63×10^{-34} J/sec) and ν_e is plasma frequency of the free electron gas (3×10^{15} sec^{-1}). The Born repulsion interaction potential can be calculated as follows:

$$V_{BR}(h) = -\frac{A\delta^6}{7560} \left[\frac{8r_p + h}{(2r_p + h)^7} + \frac{6r_p - h}{h^7} \right] \tag{4}$$

Where δ is collision diameter which in this research the collision diameter is assumed 5 Å to compare with the work done by Karoussi and Hamouda (2007) and Schembre et al. (2006). The double layer repulsion force can be calculated as:

$$V_{DLR}(h) = -\frac{\varepsilon\varepsilon_0 r_p}{4} (\Phi_{01}{}^2 + \Phi_{02}{}^2) \left\{ \left[\frac{2\Phi_{01}\Phi_{02}}{\Phi_{01}{}^2 + \Phi_{02}{}^2} \right] \ln \left[\frac{1 + \exp(-kh)}{1 - \exp(-kh)} \right] - \ln\left[1 - \exp(-2kh)\right] \right\} \tag{5}$$

In this equation, Φ_{01} and Φ_{02} are surface and particle surface potentials. The Debye length (κ) is calculated on the basis of (Israelachvili 1992):

$$\kappa = \sqrt{\frac{e^2 z^2 n_b}{\varepsilon\varepsilon_0 kT}} \tag{6}$$

Where, e is electron charge; n b is total ion density in bulk solution; z is ion valence; k is Boltzmann constant and T is temperature in K. The reported permittivity values for the water at different temperatures by Schembre et al. (2006) are interpolated to the corresponding temperatures. The surface potential (i.e. $\zeta 1$) for mineral surface ($\Phi 01$) is determined by Nernst equation and extrapolated to the corresponding temperature (Israelachvili 1992).

$$\zeta_1 = \Phi_{01} = -2.3 \left(\frac{kT}{e} \right) (pH - pH_{oi}) \tag{7}$$

$$\zeta(T) = \Phi_{01} = -0.01712\left[(T - T_o) + 1\right] \zeta(T_o) \tag{8}$$

In this equation, pH_{0i} is the iso-electric point of calcite and quartz and T is the temperature in Kelvin.

2.2 Disjoining Pressure

Basu and Sharma (1996) described the stability of water films on the basis of disjoining pressure. Disjoining pressure was expressed by Young-Laplace equation:

$$P_c = \Pi + 2\sigma_{ow} J \tag{9}$$

Where *P*c is the capillary pressure between wetting (water) and non-wetting (oil) phases (for water wet mineral), Π is the disjoining pressure in thin film, σ_{ow} is interfacial tension between oil and water, and *J* is the mean surface curvature. *J* is positive for concave surfaces and negative for convex surfaces. If the applied capillary pressure exceeds the net forces due to disjoining pressure and surface curvature, the wetting films will be unstable (Basu and Sharma 1996). The disjoining pressure is directly related to the contact angle by the following equation:

$$\cos(\theta) = 1 + \frac{1}{\sigma^{\alpha\gamma}_{\infty}} \int_0^{P_c} h d\Pi \tag{10}$$

The detail of mathematical calculation is shown in appendix. Controversial equation was reported by Karoussi

and Hamouda (2007) where they claimed that $\cos(\theta) = 1 + \frac{1}{\sigma^{\alpha\gamma}_{\infty}} \int_0^{P_c} \Pi dh$, without any mathematical derivation or justification. The reported equation in their work is dimensionally inconsistent as the dimension of derivate part is length (h or thickness of film) while the dimension of upper and lower limits of integration is pressure (p_c or capillary pressure). The stability of wetting phase can be examined by calculation of $I = \int_0^{P_c} h d\Pi$ and is discussed in appendix. Disjoining pressures could be derived from intermolecular or inter ionic forces such as van der Waals, double layer electrostatic and structural forces, which are estimated by the following equations (Israelachvili 1992):

$$\Pi_t(h) = \Pi_{LVA}(h) + \Pi_{DLR}(h) + \Pi_{BR}(h) \tag{11}$$

$$\Pi_{LVA}(h) = -\frac{A(15.96\frac{h}{\lambda} + 2)}{12\pi h^3 (1 + 5.32\frac{h}{\lambda})^2} \tag{12}$$

$$\Pi_s(h) = -A_s e^{-\frac{h}{h_s}} \tag{13}$$

$$\Pi_{DLR}(h) = nkT\left[\frac{\Phi_{r1}\Phi_{r2}\cosh(\kappa h) - \Phi_{r1}{}^2 - \Phi_{r2}{}^2}{\sinh^2(\kappa h)}\right] \tag{14}$$

$$\Phi_{ri} = \frac{e\zeta_i}{KT} \tag{15}$$

Where, h is film thickness; λ is wave length (=100 nm); A_s is structural force coefficient (1.5×10^{10} Pa); h_s is decay length (0.05 nm) and Φ_{r1} and Φ_{r2} are reduced potential for surface and particle, respectively (Israelachvili, 1992).

2.3 Relative Permeability and Capillary Pressure Model

Several experiment on core flooding showed that the maximum oil recovery occurs in neutral or slightly water-wet cores (Anderson 1985). In strongly oil-wet media, oil occupies the smallest pores, which cross ponds to high capillary pressure and high residual oil saturation. In contrast, for strongly water-wet porous media, oil become disconnected from continues oil film (snap off effect); herby trapped in pores. This results to lower oil recovery and early water breakthrough (Zhao et al. 2010). The maximum oil recovery is archived in intermediate-wet porous media, where water invades the smallest pores and oil production will continue through film flow (Hui and Blunt 2010). It is possible to speculate theoretically that, the oil saturation decreases during water/low salinity water flooding exponentially with respect to rock wettability according to Equation (16):

$$S_{or} = ae^{b\cos(\theta)} \tag{16}$$

In this equation, $S_{or}u$ is residual oil saturation after water flooding, a and b are constants and can be calculated from boundary conditions. θ is the contact angle between oil, water and mineral. If it is assumed that the rock is initially strongly oil-wet and after following with low salinity water, wettability will be altered to intermediate wetting, one can calculate the constants in Equation (16). Substituting the boundary conditions to Equation (17) yields to the following equation:

$$S_{or} = (S_{or})_f \left(\frac{(S_{or})_f}{(S_o)_i}\right)^{\cos(\theta)} \tag{17}$$

In this equation, S_{or} is the residual oil saturation, $(S_{or})_f$ is the final residual oil saturation after low salinity water flooding and $(S_o)_i$ is the initial oil saturation in the rock. Assuming the definition of normalized oil saturation and Corey correlation for calculation of normalized relative permeability and capillary pressure, it is possible to write:

$$S_{on} = \frac{s_o - s_{or}}{1 - s_{or} - s_{wi}} \tag{18}$$

$$k_{ro} = \left[\frac{S_o - (S_{or})_f \left(\frac{(S_{or})_f}{(S_o)_i}\right)^{\cos(\theta)}}{1 - (S_{or})_f \left(\frac{(S_{or})_f}{(S_o)_i}\right)^{\cos(\theta)} - S_{wi}} \right]^{\frac{2+\lambda}{\lambda}} \tag{19}$$

$$k_{rw} = \left[1 - \left(\frac{S_o - (S_{or})_f \left(\frac{(S_{or})_f}{(S_o)_i}\right)^{\cos(\theta)}}{1 - (S_{or})_f \left(\frac{(S_{or})_f}{(S_o)_i}\right)^{\cos(\theta)} - S_{wi}} \right) \right]^{\frac{2+3\lambda}{\lambda}} \tag{20}$$

$$P_C = P_C^{\,th} \left[1 - \left(\frac{S_o - (S_{or})_f \left(\frac{(S_{or})_f}{(S_o)_i}\right)^{\cos(\theta)}}{1 - (S_{or})_f \left(\frac{(S_{or})_f}{(S_o)_i}\right)^{\cos(\theta)} - S_{wi}} \right) \right]^{\frac{-1}{\lambda}} \tag{21}$$

Where $P_C^{\,th}$ and λ are capillary threshold and pore size distribution, respectively. Similar approach were reported in the literature to model continues wettability alteration during immiscible CO_2 flooding (Al-Mutairi et al. 2012).

3. Results and Discussion

This section is dividing in three subsections. The first part addresses the calculation procedures of contact angle and discusses the influences of ions and temperature on wettability alteration. Total potential interactions between modified minerals and different ions are discussed in the second part, while the last section is dealing with mathematical modeling of relative permeability and capillary pressure from contact angle.

3.1 Modeling of Contact Angle and Subsequent Effects of Ions and Temperature

Before addressing the stability of water film for modified minerals by asphaltene in presence of different ions, the Hamaker constant is computed for different temperatures in accordance with Lifshitz theory for ternary system of mineral/water/oleic. In Figure 1, the variation of Hamaker constant versus temperature is shown for quartz and calcite minerals. The used dielectric properties of three media and refractive index corresponding to the media are shown in Table 1.

Table 1. Dielectric properties and refractive index values for mineral /water/ toluene systems (Israelachvili 1992)

Calcite/Water/Toluene					
Media 1	Calcite	n_1	1.638	ε_1	8
Media 2	Toluene	n_2	1.496	ε_2	2.38
Media 3	Water	n_3	1.323	ε_3	80.1
Quartz/Water/Toluene					
Media 1	Quartz	n_1	1.536	ε_1	4.29

Media 2	Toluene	n_2	1.496	ε_2	2.38
Media 3	Water	n_3	1.323	ε_3	80.1

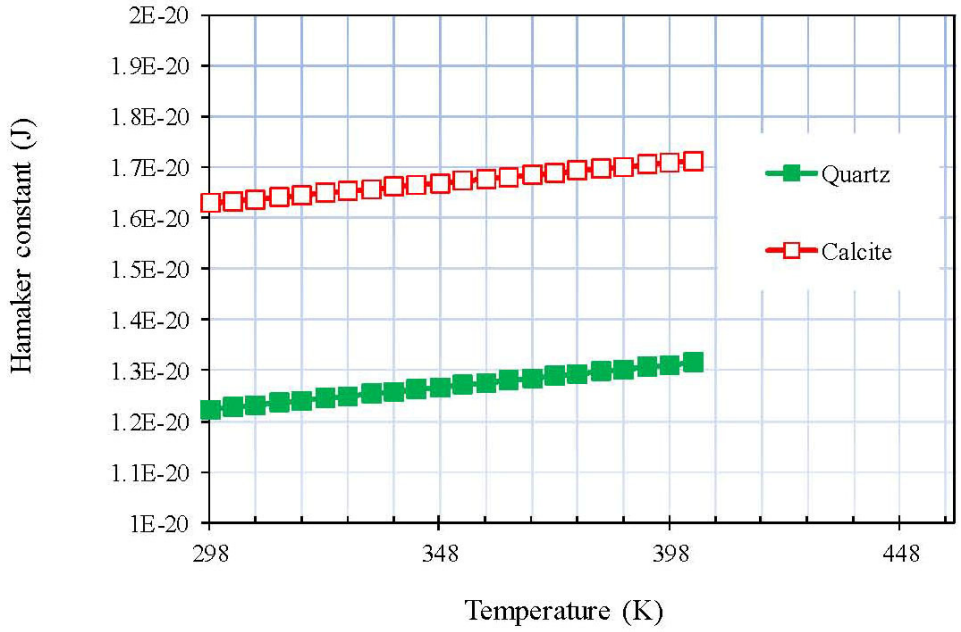

Figure 1. The variation of Hamaker constant versus temperature for quartz/water/toluene and calcite/water/toluene systems

From Figure 1, it is clear that the Hamaker constants for calcite and quartz are increasing linearly with the temperature. However these trends for calcite (≈7.98E-24 J/K) and quartz (≈8.77E-24 J/K) are slightly different. This can be also observed from Equation (22) in which the derivate of Hamaker coefficient to the temperature is a constant and is equal to:

$$\frac{dA}{dT} = \frac{3}{4}k\left(\frac{\varepsilon_1 - \varepsilon_3}{\varepsilon_1 + \varepsilon_3}\right)\left(\frac{\varepsilon_2 - \varepsilon_3}{\varepsilon_2 + \varepsilon_3}\right) \tag{22}$$

This is in contrast of the trend reported by Karoussi and Hamouda (2007) where they showed that Hamaker coefficient for calcite/decane/water system is decreasing by increasing temperature. Lifshitz theory has been used in their work to calculate the Hamaker constant; however the method of calculation (or simplification) for the second term ($\frac{3\hbar}{4\pi}\int_{\nu_1}^{\infty}\left(\frac{\varepsilon_1(\nu)-\varepsilon_3(\nu)}{\varepsilon_1(\nu)+\varepsilon_3(\nu)}\right)\left(\frac{\varepsilon_2(\nu)-\varepsilon_3(\nu)}{\varepsilon_2(\nu)+\varepsilon_3(\nu)}\right)d\nu$) was not mentioned. Equation (22) shows that sign of $\frac{dA}{dT}$ is dependent to the values of ε_1, ε_2 and ε_3. As the dielectric constant of water (ε_3) is larger than the dielectric constant of calcite or normal decane (ε_1 and ε_2) so $\frac{dA}{dT}$>0; then the Hamaker constant could not decrease by increasing temperature.

The stability of water film in calcite/silicate system (modified with 0.35 wt. % asphaltene) in presence of distilled water (DW), 0.1 M NaCL, 0.1 M Na_2SO_4 and 0.1 M $MgCl_2$ is addressed in this section. Jada et al. (2002) and Rezaei Gomari et al. (2006a) reported the zeta potential charge of quartz and calcite as a function of pH. Parra- Barraza et al. (2003) also reported the zeta potential of asphaltene versus pH when the asphaltene is precipitated from crude oil in presence of n-heptane with the ratio of 1 to 40. In Figure 2, calculated disjoining pressure as a function of water film thickness at 25 ^{o}C for quartz and calcite is demonstrated. From Figure 2a) it can be seen that water film over silicate mineral in presence of asphaltene dissolved in toluene and DW or 0.1 M Mg^{2+} is unstable since the area under disjoining capillary pressure is less than $-\sigma^{\alpha\gamma}{}_{\infty}$ (Type 3 according to

appendix); hence the system is strongly oil-wet. The water film for quartz/0.1 M SO_4^{2-}/asphaltene or quartz/0.1 M NaCl/ asphaltene is meta-stable (Type 2 according to appendix) and the system is more water-wet respect to quartz/0.1 M Mg^{2+}/asphaltene or quartz/DW/ asphaltene. As it can be seen in Figure 2 b, for calcite, the water film is unstable regardless to the type of ions; however the instability of water-film over calcite in presence of 0.1 M Mg^{2+} and 0.1 M SO_4^{2-} is in lesser extent compared to 0.1 M NaCl and DW.

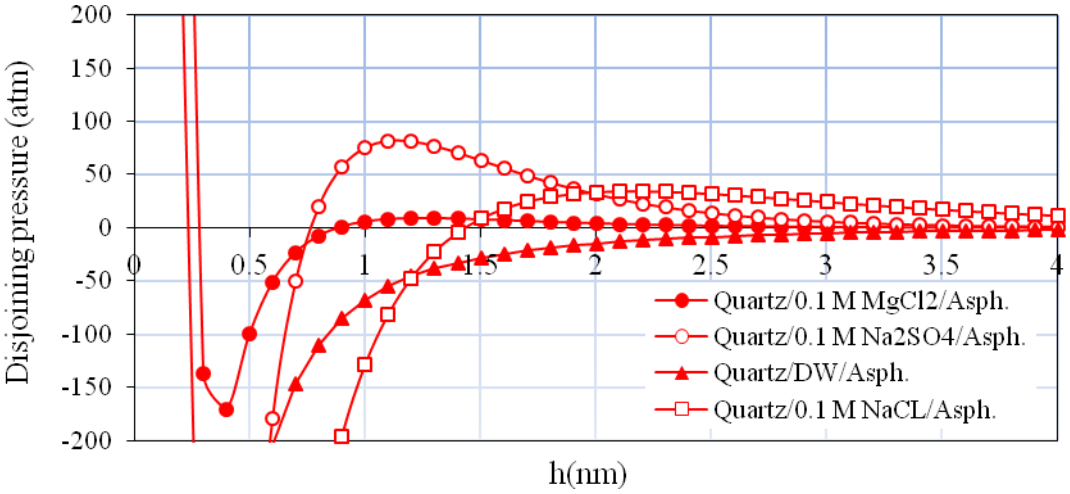

a) Quartz

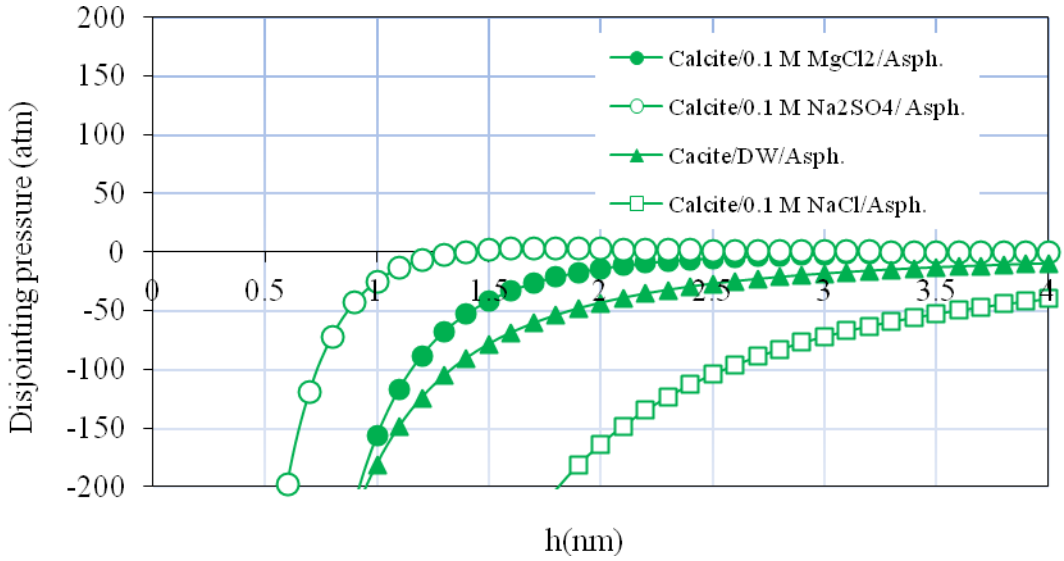

b) Calcite

Figure 2. Calculated disjoining pressure as a function of water film thickness at 25 °C for a) quartz and b) calcite in presence of distilled water (DW), 0.1 M NaCl, 0.1 M Na_2SO_4 and 0.1 M $MgCl_2$

In Figure 3, disjoining pressure as a function of water film thickness at 25 °C for quartz and calcite in presence of low salinity and synthetic sea water is shown. The ionic composition of low salinity seawater is obtained by 1000 times diluting the concentration of ions in seawater. In Table 2, the ionic composition of synthetic seawater and low salinity seawater is shown.

Table 2. Ionic composition of synthetic sea water and low salinity sea water

Ions	Concentration (mol/l)	Concentration (mol/l)
	Synthetic Sea Water	Low Salinity Water
NaCl	0.4	0.0004
KCl	0.01	0.00001
$CaCl_2$ ($2H_20$)	0.013	0.000013
$MgCl_2$($6H_20$)	0.045	0.000045
$NaHCO_3$	0.002	0.000002
Na_2(SO_4)	0.024	0.000024
TDS	0.494	0.000494

From Figure 3, it can be seen that water film over silicate and calcite minerals in presence of asphaltene dissolved in toluene and synthetic sea water (SSW) is unstable as the area under disjoining capillary pressure is less than $-\sigma^{\alpha\gamma}{}_{\infty}$ (Type 3); hence the system is strongly oil-wet. The water film for both types of minerals (quartz and calcite) in presence of low salinity water (LSW) and asphaltene is meta-stable (Type 2) and the contact angle forms between zero and 90°. This shows that LSW may alter the wettability of calcite and silicate minerals toward water wet condition. Mahani et al. (2014) also observed a wettability alteration process toward less oil wet condition when clay coated silica glass is exposed to low salinity brine with slow kinetic reaction (Mahani et al. 2014). They addressed that the time scale of wettability alteration is ten to twenty times longer than expected time by diffusion (Mahani et al. 2014). It seems to be that the kinetic of the process is consistent to the electro kinetic ion diffusion mechanism involving DLVO forces between oil layer, water film and clay minerals.

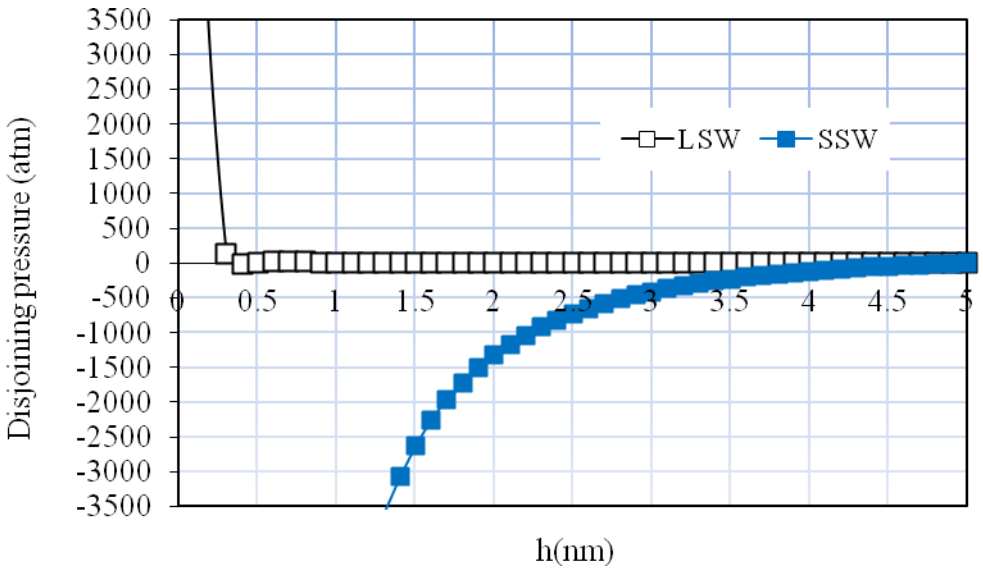

a) Quartz

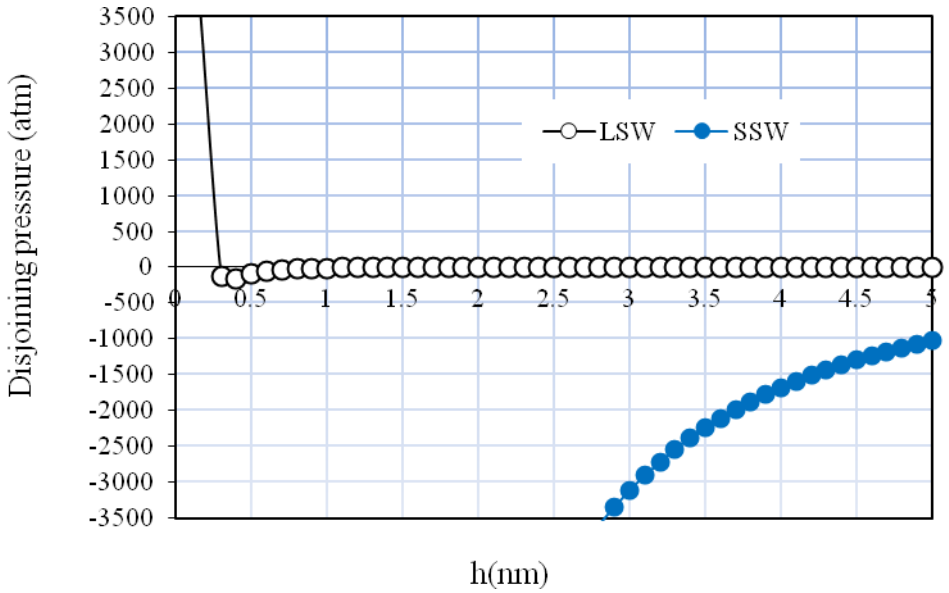

b) Calcite

Figure 3. Calculated disjoining pressures as a function of water film thickness at 25 °C for a) quartz and b) calcite in presence of low salinity water (LSW) and synthetic sea water (SSW)

Static contact angle between n-decane, distilled water and aged mineral (prewetted with distilled water (DW), 0.1 M NaCL, 0.1 M Na_2SO_4 and 0.1 M $MgCl_2$ and 0.35 wt. % dissolved asphaltene in toluene, are calculated based on Equation (16) and shown and compared in Table 3 with experimental values reported by Alipour Tabrizy et al. (2011b) and Mahani et al. (2014). The experimental error measurement was reported within 3° and 5° by Alipour Tabrizy et al. (2011b) and Mahani et al. (2014), respectively.

Table 3. Contact angle between oil (n-decane), distilled water and aged mineral (pre wetted with distilled water (DW), 0.1 M NaCL, 0.1 M Na_2SO_4 and 0.1 M $MgCl_2$ and 0.35 wt. % dissolved asphaltene in toluene at 25 °C

Modification brine	0. 1 M Mg^{2+}	DW	0. 1 M SO_4^{2-}	0. 1 M NaCL	LSW	SSW
Quartz						
Theoretical calculation	120	109	93	97	60	93
Experimental **	133	95	90	93		
Experimental *					67	90
Calcite						
Theoretical calculation	78	105	120	95	80	140
Experimental *	65	100	127	95		

*From Alipour Tabrizy et al. (2011b).

**From Mahani et al. (2014).

The effect of temperature on disjoining pressure has been shown in Figure 4. for quartz/0.1 M Mg^{2+}/asphaltene and calcite/0.1 M Mg^{2+}/asphaltene systems for temperatures 25 °C and 130 C°. Temperature has two main effects on calculated disjoining pressure, the first effect is related to Hamaker constant and the second effect is related to zeta potential of surface mineral and asphaltene colloids which they control the double layer interaction force. For both systems, increasing the temperature is enhancing the stability of water film over mineral surface; hence it will improve the hydrophilicity of system. The contact angle is decreasing from 77.78° to 31.78 ° for calcite mineral and from 124.75 ° to 16.25 ° for quartz mineral by increasing of temperature from 25 C° to 130 C°. This indicates the influences of ions on water film stability are accelerated by increasing temperature both for

carbonate and silicates mineral.

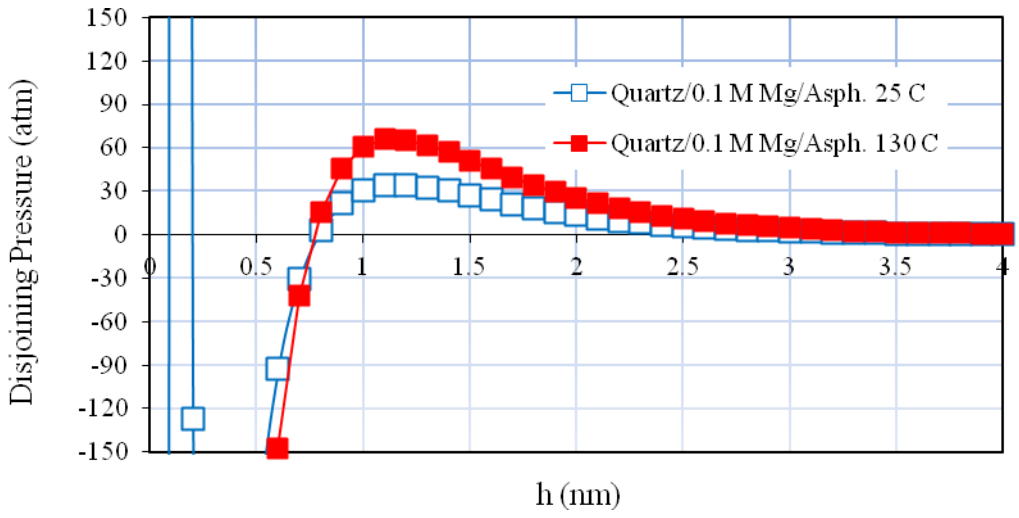

a) Quartz

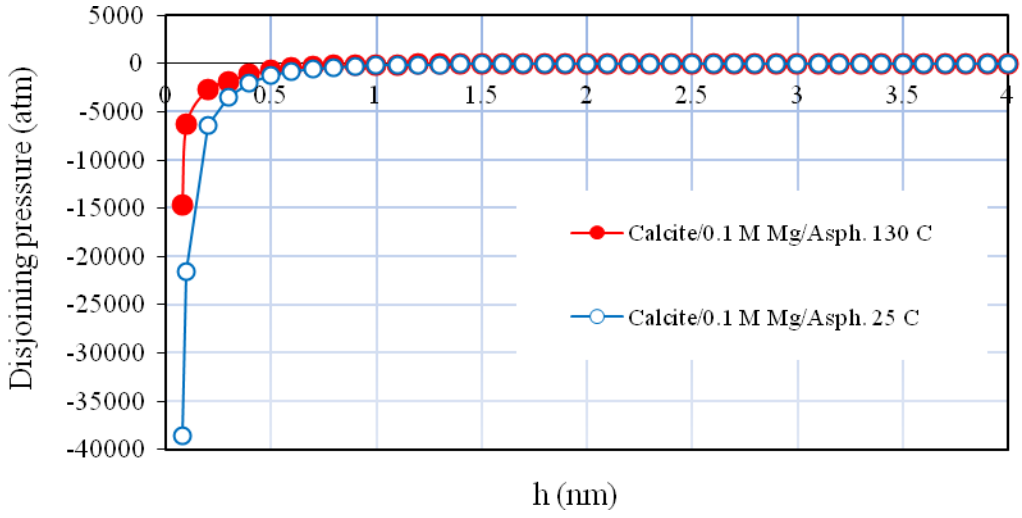

b) Calcite

Figure 4. Calculated disjoining pressure as a function of water film thickness and temperature for a) quartz and b) calcite in presence 0.1 M $MgCl_2$

3.2 Total Potential Interactions between Modified Minerals and Different Ions

Total interaction potential can be used to order the affinity of different ions/polar components to adsorb to the mineral surface. The calculation of total interaction potential for quartz and calcite are shown in Figure 5. From this figure it is possible to see that for modified quartz with asphaltene in presence of distilled water (DW), 0.1 M NaCL, 0.1 M Na_2SO_4 and 0.1 M $MgCl_2$, the total interaction potential between asphaltene colloids and mineral surface are always positive; hence the interaction force between asphaltene colloids and mineral surfaces is repulsive. However the magnitude of this force is dependent to the type of brine, where for 0.1 M NaCL and 0.1 M Na_2SO_4 this repulsion is more pronounced; hence the modified quartz with asphaltene in presence of 0.1 M NaCl and 0.1 M Na_2SO_4 are more water-wet comparing to the modified quartz with asphaltene in presence of

DW and 0.1 M $MgCl_2$. For modification of quartz by asphaltene in presence of 0.1 M $MgCl_2$, Mg^+ ions may act as bridge between asphaltene and quartz surfaces. This calculation is supported by water vapor adsorption and contact angle measurements by Alipour Tabrizy et al. (2011b) and is in agreement with pervious research works reported by Chukwudeme and Hamouda (2009) and Morrow et al. (2000). They explained in different experiments, possible bridging as an explanation. In other flooding experiments in micro model tests (Liu et al. 2010) for enhanced heavy oil recovery by alkaline flooding; it was found that oil recovery was greatly affected by wettability alteration of water-wet grains to preferentially oil-wet due to magnesium ion bonding. For calcite, the potential interaction between calcite and asphaltene in presence of DW and 0.1 M NaCL are negative which supports the high affinity of calcite and carbonate mineral to adsorb asphaltene. Calcite and carbonate minerals modified by asphaltene are strongly oil-wet compared to silicate minerals since the interaction potential is negative and the interaction force between asphaltene and calcite mineral surfaces is attractive unlike asphaltene and quartz minerals. Figure 5b) shows 0.1 M Mg^{2+} ions can enhance strongly the hydrophilicity of modified calcite with asphaltene as the affinity of asphaltene to interlock with Mg^{2+} is much less than Ca^{2+}. The total interaction potential between asphaltene colloids and Ca^{2+} is smaller that in two orders of magnitude compared to asphaltene colloids and Mg^{2+}. It has been reported previously that the affinity of cations to adsorb negatively charged colloidal particles (e.g. asphaltene) has the following order: (Tang and Morrow 1999)

$Li^+ < Na^+ < K^+ < Mg^{2+} < Ca^{2+} < H^+$

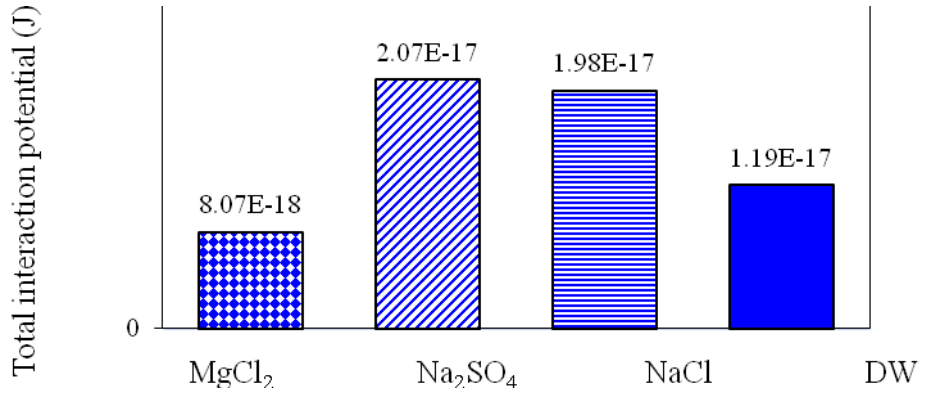

a) Quartz

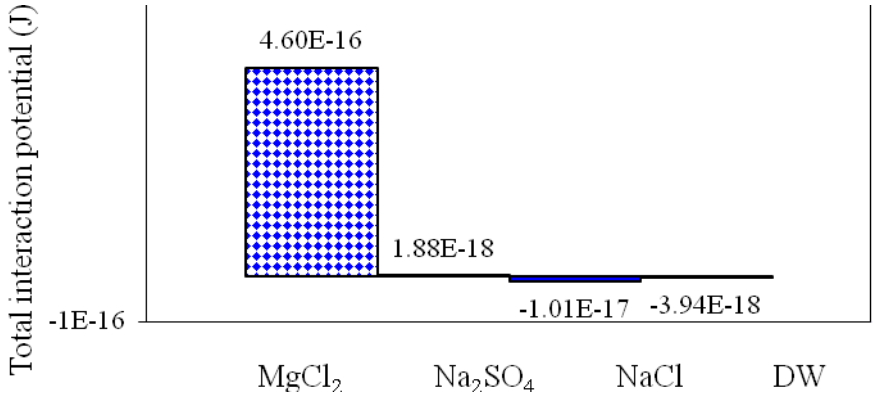

b) Calcite

Figure 5. Calculated total interaction potential between asphaltene colloids, quartz and calcite in presence of distilled water (DW), 0.1 M NaCl, 0.1 M Na_2SO_4 and 0.1 M $MgCl_2$

The calculations of total interaction potential are shown also for synthetic seawater and low salinity seawater for quartz, calcite and asphaltene colloidal systems in this subsection. The total interaction potential of quartz and /or calcite, synthetic sea water (SSW) and low salinity sea water (LSW), asphaltene colloids are demonstrated in Figure 6. In quartz/brine/asphaltene system, the total interaction potential is slightly positive for DW and SSW. For LSW, the total interaction potential is considerably larger than DW and SSW (10^3 order of magnitude larger that SSW and 10^2 order of magnitude larger than DW). In calcite/brine/asphaltene system, the total interaction potential is negative (attractive) for DW and SSW. For LSW, the total interaction potential is positive (repulsive). This clearly shows the applicability of low salinity seawater for tertiary improved oil recovery after sea water injection both for sandstone and carbonate reservoir rocks. The low salinity seawater flooding makes the crude oil/brine/rock (COBR) system more water-wet; hence it can produce additional oil between 5% up to 15% from water flooded sandstone and carbonate rocks (Tang and Morrow 1999).

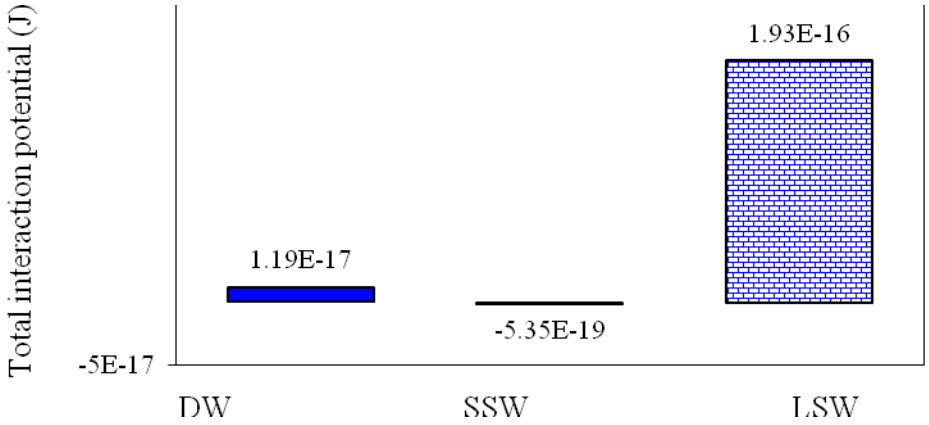

a) Quartz

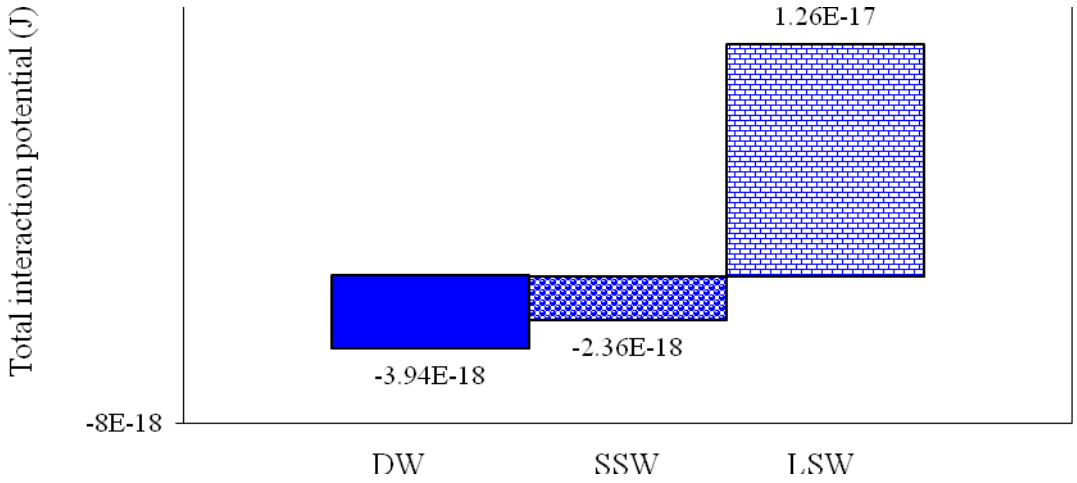

b) Calcite

Figure 6. Calculated total interaction potential between asphaltene colloids, quartz and calcite in presence of distilled water (DW), Synthetic Sea Water (SSW) and Low Salinity Sea Water (LSW)

3.3 Modeling of Relative Permeability and Capillary Pressure

Figure 7 shows the relative permeability and capillary pressure curves from estimated contact angles by applying Equation (19) till Equation (21) for a sandstone rock saturated initially with 0.35 wt. % dissolved asphaltene in toluene and flooded with low salinity water (LSW), synthetic sea water (SSW) and 0.1 M $MgCl_2$. Capillary threshold and pore size distribution for this rock sample is assumed as 2.5 bar and 0.5 respectively.

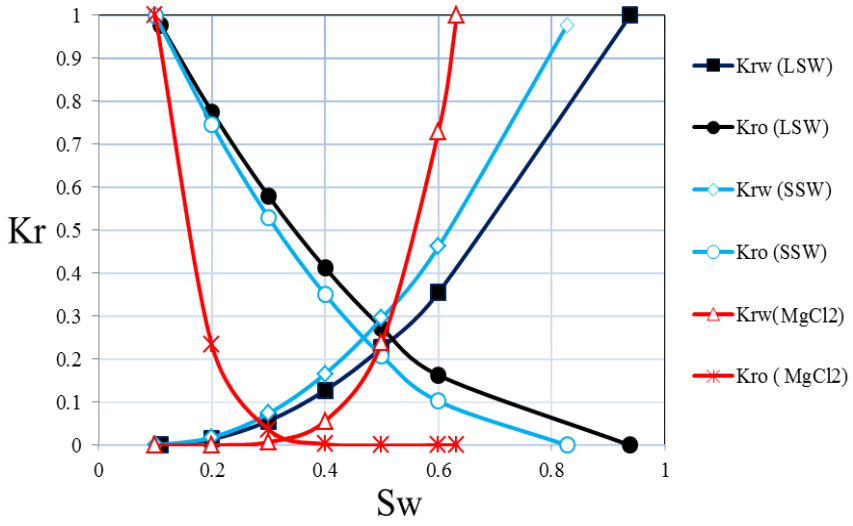

a) Relative permeability

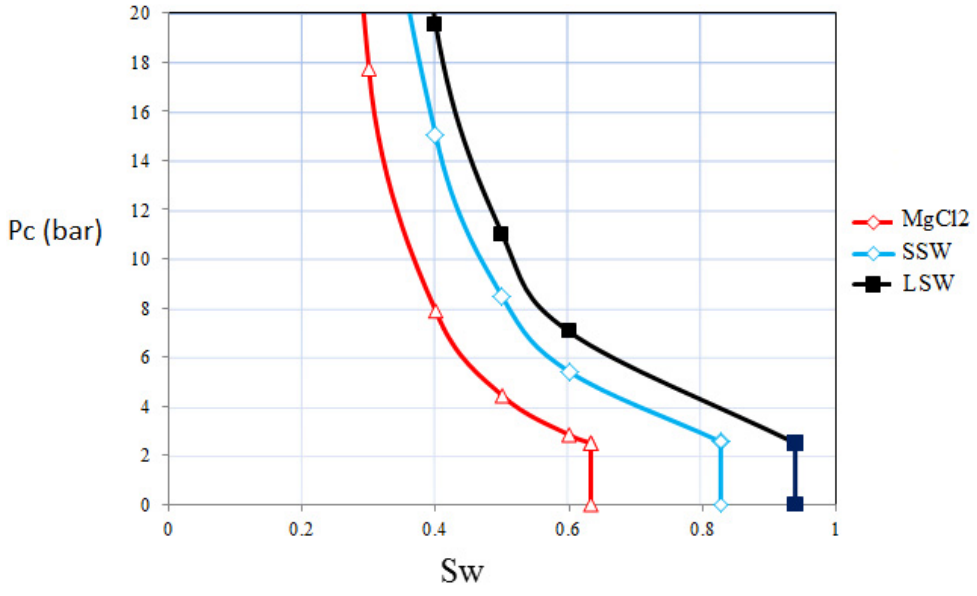

b) Capillary pressure

Figure 7. Calculated relative permeability and capillary pressure curves from contact angle for sandstone rock saturated with 0.35 wt. % dissolved asphaltene in toluene and flooded with low salinity water (LSW), synthetic sea water (SSW) and 0.1 M $MgCl_2$

Two observations can be seen from Figure 7. The first observation is the shift of the oil relative permeability toward the right hand side and a decrease in residual oil saturation with reduction of contact angle for the core flooded with low salinity water (LSW). This indicates oil becomes confined to smallest pores as the rock is

altered from strongly oil wet to intermediate wet condition. On the other hand, water relative permeability decreases as the rock wetting state is altered towards intermediate wet condition during low salinity water (LSW) injection. The crossover point for oil/water relative permeability curves is located at 0.5 of S_w for the core flooded with low salinity water, whereas for the core flooded with synthetic sea water and 0.1 M $MgCl_2$, the crossover points are located at 0.4 and 0.3 respectively. The second observation is related to the area of the capillary pressure curves for the sandstone rock saturated with 0.35 wt. % dissolved asphaltene in toluene and flooded with different brines. Figure 7b demonstrates the area below capillary pressure curve (work per unit volume of rock to displace water by oil) is higher for flooded core with low salinity water (LSW) compared to that for flooded core with sea water or 0.1 M $MgCl_2$. This also shows the wettability alteration of sandstone rock towards intermediate wetting condition during low salinity water flooding.

4. Conclusions

This paper provides insights to a more fundamental understating of oil recovery by water/low salinity water flooding in silicates and carbonate rocks. An approach is discussed to assess the reservoir rock wettability (contact angle) from oil and mineral surface chemistry properties, ions concentration, pH and temperature. A model for evaluating relative permabilities and capillary pressure is used also to describe the wettability alteration mechanism and estimates the flooding/imbibition recovery by different ions.

The wettability change to a less oil-wet condition was shown for both types of sandstone and carbonate reservoirs during low salinity water; however the wettability alteration is more pronounced for modified silicate mineral compared to modified calcite mineral. Increasing the temperature also enhances the stability of the water film around the mineral surface and increases the efficiency of low salinity water flooding. The model shows also Mg^{2+} ion enhances the hydrophilicity characteristics for oil-wet calcite mineral while for oil-wet silicate surface, SO_4^{2-} ion enhances the hydrophobicity behaviour. This is consistent to the experimental observations reported in the literature; however it is worth mention that the physics underlying water/low salinity flooding is more complex than the simple model presented in this work, among them geomechanical considerations of rock during water/low salinity flooding (such as dissolution, precipitation, compaction and clay swelling) should receive considerable attention.

Acknowledgments

Authors declare no other competing interests. The paper reflects only the viewpoints of authors and not their corresponding organizations by any means.

References

Akin, S., Schembre, J. M., Bhat, S. K., & Kovscek, A. R. (2000). Spontaneous imbibition characteristics of diatomite. *Journal of Petroleum Science and Engineering, 25*, 149-165. http://dx.doi.org/10.1016/S0920-4105(00)00010-3

Alipour, T. V., Denoyel, R., & Hamouda, A. A. (2011a). Characterization of wettability modification of calcite, quartz and kaolinite: Surface energy analysis. *Colloid and Surface A., 384*, 98-108. http://dx.doi.org/10.1016/j.colsurfa.2011.03.021

Alipour, T. V., Hamouda, A. A., & Denoyel, R. (2011b). Influence of sulfate and magnesium ions on wettability alteration of calcite, quartz and kaolinite: Surface energy analysis. *Energy & Fuels, 25*, 1667-1680. http://dx.doi.org/10.1021/ef200039m

Al-Mutairi, S. M., Abu-khamsin, S. A., & Hossain, M. E. (2012). A Novel approach to handle continuous wettability alteration during immiscible CO2 flooding process. *Abu Dhabi International Petroleum Conference and Exhibition*, 11-14 November, Abu Dhabi, UAE. http://dx.doi.org/10.2118/160638-MS

Anderson, W. G. (1986). Wettability literature survey: Part 1. Rock /oil/ brine interactions and the effects of core handling on wettability. *Journal of Petroleum Technology, 38*, 1125-1144. http://dx.doi.org/10.2118/13932-PA

Austad, T., Shariatpanahi, F., Starnd, S., Black, C. J. J., & Webb, K. J. (2012). Conditions for a low-salinity enhanced oil recovery (EOR) effect in carbonate oil reservoirs. *Energy & Fuels, 26*, 569-575. http://dx.doi.org/10.1021/ef201435g

Babadagli, T. J. (2000). Evaluation of EOR methods for heavy oil recovery in naturally fractured reservoirs. *Journal of Petroleum Science and Engineering, 37*, 25-37. http://dx.doi.org/10.1016/S0920-4105(02)00309-1

Basu, S., & Sharma, M. M. (1996). Measurement of critical disjoining pressure for dewetting of solid surfaces.

Colloid and Surface A., 181, 443-455. http://dx.doi.org/10.1006/jcis.1996.0401

Chukwudeme, E. A., & Hamouda, A. A. (2009). Oil recovery from polar components (asphaltene and SA) treated chalk rocks by low salinity water and water containing SO_4^{2-} and Mg^{2+} at different temperatures. *Colloids Surface A., 336*, 174-182. http://dx.doi.org/10.1016/j.colsurfa.2008.11.051

Freitas, A., & Sharma, M. (2001). Detachment of particles from surfaces: An AFM study. *Journal of Colloid and Interface Science, 233*, 73-82. http://dx.doi.org/10.1006/jcis.2000.7218

Giasson S, Kuhl, T., & Israelachvili, J. N. (1989). Adsorption and interaction forces of micellar and microemulsion solutions in ultrathin films. *Langmuir, 14*, 891-898. http://dx.doi.org/10.1021/la960747w

Grasso, D., Subramaniam, K., Butkus, M., Strevett, K., & Bergendahl, J. (2002). A review of non-DLVO interactions in environmental colloidal systems. *Reviews in Environmental Science and Bio Technology, 1*, 17-38. http://dx.doi.org/10.1023/A:1015146710500

Hamouda, A. A., & Karoussi, O. (2008). Effect of temperature, wettability and relative Permeability on oil recovery from oil-wet chalk. *Energies, 1*, 19-23. http://dx.doi.org/10.3390/en1010019

Hamouda, A. A., & Rezaei G. K. A. (2006). Influence of temperature on wettability alteration of carbonate reservoirs. *SPE/DOE Symposium on Improved Oil Recovery*, Tulsa, OK, April 22–26. http://dx.doi.org/10.2118/99848-MS

Hamouda, A. A., & Valderhaug, O. M. (2014). Investigating enhanced oil recovery from sandstone by low salinity water and fluid/rock Interaction. *Energy & Fuels, 28*, 898-908. http://dx.doi.org/10.1021/ef4020857

Hui, M. H., & Blunt, M. J. (2000). Effects of wettability on three-phase flow in porous media. *Journal of Physical Chemistry B., 104*, 3833-3845. http://dx.doi.org/10.1021/jp9933222

Israelachvili, J. N. (1998). *International and Surfaces Forces* (2nd ed.). Academic Press.

Jada, A., Choau, A., Bertrand, Y., & Moreau, O. (2002). Adsorption and surface properties of isolating oils. *Fuel, 81*, 1227-1232. http://dx.doi.org/10.1016/S0016-2361(02)00019-4

Jucker, B., Zehnder A., & Harms, H. (1998). Quantification of polymer interactions in bacterial adhesion. *Environmental Science and Technology, 32*, 2909-2915. http://dx.doi.org/10.1021/es980211s

Karoussi, O., & Hamouda, A. A. (2007). Imbibition of sulfate and magnesium ions into carbonate rocks at elevated temperatures and their influence on wettability alteration and oil recovery. *Energy & Fuels, 21*(4), 2138-2146. http://dx.doi.org/10.1021/ef0605246

Lager, A., Webb, K. J., & Black, C. J. J. (2007). Impact of brine chemistry on oil recovery. *14th European Symposium on Improved Oil Recovery*, Cairo, Egypt.

Legens, C., Toulhoat, H., Cuiec, L., Villieras, F., & Palermo, T. (1998). Wettability change related to the Adsorption of organic acids on calcite: Experimental and Ab initio computational studies (pp. 27-30). *SPE Annual Technical Conference and Exhibition*, New Orleans, September. http://dx.doi.org/10.2118/49319-MS

Liu, Q., Dong, M., Asghari, K., & Tu, Y. (2010). Wettability alteration by magnesium ion binding in heavy oil/brine/chemical/sand systems - analysis of hydration forces. *Natural Science, 2*(5), 450-456. http://dx.doi.org/10.4236/ns.2010.25055

Loahardjo, N., Xie, X., Yin, P., & Morrow, N. R. (2007). Low salinity water flooding of a reservoir rock, *SCA*, 29.

Mahani, H., Berg, S., Ilic, D., Bartels , W. B., & Joekar-Niasar V. (2014). Kinetics of low salinity flooding effect. *SPE Journal,* 1-13.

Mahani, H., Sorop, D., Ligthelm, D. J., Brooks, D., Vledder, P., Mozahem, F., & Ali, Y. (2011). Analysis of field responses to low-salinity water flooding in secondary and tertiary mode in Syria, SPE EUROPEC/EAGE Annual Conference and Exhibition, 23-26 May, Vienna, Austria. http://dx.doi.org/10.2118/142960-MS

McGuire, P. L., Chatham, J. R., Paskvan, F. K., Sommer, D. M., & Carini, F. H. (2005). Low salinity oil recovery: An exciting new EOR opportunity for Alaska's North Slope. *SPE Western Regional Meeting*, Irvine, CA. http://dx.doi.org/10.2118/142960-MS

Morrow, N. R., Lim, H. T., & Ward, J. S. (1986). Effect of crude-oil-induced wettability changes on oil recovery. *SPE Formation and Evaluation*, 89-103. http://dx.doi.org/10.2118/13215-PA

Oss, C. V. (1994). Interfacial forces in aqueous media. Marcel Dekker, New York.

Parra, B. H., Hernandez, M. D., Lizardi, J., Herna´ndez, J., Herrera, U. R., & Valdez, M. (2004). The zeta potential and surface properties of asphaltene obtained with different crude oil/n-heptane proportions. *Fuel*, *82*, 869-874. http://dx.doi.org/10.1016/S0016-2361(03)00002-4

Petrovich, R., & Hamouda, A. A. (1989). Dolomitization of Ekofisk oil field reservoir chalk by injected seawater. In Arehart, G. B., & Hulston, J. R. (Eds.), *Water-Rock Interaction* (pp. 345-348), Balkema, Rotterdam.

Rezaei, D. A., Puntervold, T., & Austad. T. (2011). Chemical verification of the EOR mechanism by using low saline/smart water in sandstone. *Energy & Fuels, 25*, 2151–2162. http://dx.doi.org/10.1021/ef200215y

Rezaei, G. K. A., Denoyel, R., & Hamouda, A. A. (2006b). Wettability of calcite and mica modified by different long chain fatty acids (C18 acids). *Journal of colloid and interface science, 297*, 470-479. http://dx.doi.org/10.1016/j.jcis.2005.11.036

Rezaei, G. K. A., & Hamouda, A. A. (2006c). Effect of fatty acids water composition and pH on the wettability alteration of calcite surface. *Journal of Petroleum Science and Engineering, 50*, 140-150. http://dx.doi.org/10.1016/j.petrol.2005.10.007

Rezaei, G. K. A., Hamouda, A. A., & Denoyel, R. (2006a). Influence of sulfate ions on the interaction between fatty acids and calcite surfaces. *Colloids Surface A., 287*, 29-35. http://dx.doi.org/10.1016/j.colsurfa.2006.03.018

Rijnaarts, H., Norde, W., Lyklema, J., & Zehnder, A. (1999). DLVO and steric contributions to bacterial deposition in media of different ionic strengths. *Colloids and Surfaces B: Bio interfaces, 14*, 179-195. http://dx.doi.org/10.1016/S0927-7765(99)00035-1

Schembre, J. M., Tang, G. Q., & Kovscek, A. R. (2006). Wettability alteration and oil recovery by water imbibition at elevated temperatures. *Journal of Petroleum Science and Engineering, 52*, 131-148. http://dx.doi.org/10.1016/j.petrol.2006.03.017

Tang, G. Q., & Morrow, N. R. (1999). Influence of brine composition and fines migration on crude oil/brine/rock interactions and oil recovery. *Journal of Petroleum Science and Engineering, 24*, 99-111. http://dx.doi.org/10.1016/S0920-4105(99)00034-0

Zhao, X., Blunt, M. J., & Yao, J. (2010). Pore-scale modeling: Effects of wettability on water flood oil recovery. *Journal of Petroleum Science and Engineering, 71*, 169-178. http://dx.doi.org/10.1016/j.petrol.2010.01.011

Zhou, X., Morrow, N. R., & Ma, S. (2000). Interrelationship of wettability, initial water saturation, aging time, and oil recovery by spontaneous imbibition and water flooding. *SPE Journal, 5*(2), 199-207. http://dx.doi.org/10.2118/62507-PA

Appendix

The disjoining pressure is expressed in terms of the change in the sum of interfacial tensions of the surrounding surfaces with respect to its thickness (Basu and Sharma, 1996). This can be expressed as:

$$\Pi = -\frac{\partial(\sigma^{\alpha\gamma} + \sigma^{\beta\gamma})}{\partial h}\Big|_{@T} \tag{A.1}$$

Where $\sigma^{\alpha\gamma}{}_{\infty}, \sigma^{\beta\gamma}{}_{\infty}$ the interfacial tensions for thin fluid films and h is the film thickness. By integration of this equation, the critical pressure is calculated as:

$$(\sigma^{\alpha\gamma} + \sigma^{\beta\gamma}) - (\sigma^{\alpha\gamma}{}_{\infty} + \sigma^{\beta\gamma}{}_{\infty}) = -\int_{\infty}^{h(P_c)} \Pi dh \tag{A.2}$$

Where $\sigma^{\alpha\gamma}{}_{\infty}, \sigma^{\beta\gamma}{}_{\infty}$ are bulk interfacial tensions between liquids and solid surface. $h(P_c)$ is the film thickness at capillary pressure. The final film tension is:

$$\sigma^{f} = \sigma^{\alpha\gamma} + \sigma^{\beta\gamma} + \Pi h \tag{A.3}$$

Where, Π is disjoining pressure at film thickness h. By applying Equation (A.2) the following relation is obtained:

$$\sigma^f = (\sigma^{\alpha\gamma}{}_{\infty} + \sigma^{\beta\gamma}{}_{\infty}) - \int_{\infty}^{h(P_c)} \Pi dh + \Pi h \tag{A.4}$$

Using the derivative chain rule, the following equation can be written:

$$\sigma^f = (\sigma^{\alpha\gamma}{}_{\infty} + \sigma^{\beta\gamma}{}_{\infty}) - \int_{0}^{P_c} h d\Pi \tag{A.5}$$

The contact angle can be expressed as applying force balance calculation:

$$\cos(\theta) = \frac{\sigma^f - \sigma^{\beta\gamma}{}_{\infty}}{\sigma^{\alpha\gamma}{}_{\infty}} \tag{A.6}$$

Hence; the disjoining pressure is directly related to the contact angle by the following equation:

$$\cos(\theta) = 1 + \frac{1}{\sigma^{\alpha\gamma}{}_{\infty}} \int_{0}^{P_c} h d\Pi u \tag{A.7}$$

One can divide the variation of disjoining pressure curve versus film thinness in three cases. In the first case (Type 1), the area under disjoining pressure versus film thinness curve is positive or zero ($I \geq 0$); accordingly the wetting phase is stable and cannot create an angle (or zero contact angle) between solid surface and two liquid phases. In the second case (Type 2), the area under disjoining pressure versus film thinness curve is between zero and $-\sigma^{\alpha\gamma}{}_{\infty}$ ($-\sigma^{\alpha\gamma}{}_{\infty} \leq I \leq 0$) where the wetting phase is meta-stable and the contact angle between zero and 90^o is created. In the third case (Type 3), the area under disjoining pressure versus film thinness curve is less than $-\sigma^{\alpha\gamma}{}_{\infty}$ ($-2\sigma^{\alpha\gamma}{}_{\infty} \leq I \leq -\sigma^{\alpha\gamma}{}_{\infty}$) and the wetting phase is unstable with the contact angle between 90^o and 180^o.